Selection of CMIP6 representative climate models and downscaling in Northern Nigeria

Idris Muhammad Wada (wada@fuwukari.edu.ng)
Hohai University
Haruna Shehu Usman
Bayero University
S. Nwankwegu Amechi
Southwest University
Nwunuji Usman Makhai
Federal University Wukari
Haftu Gebresellase Selamawit
Hohai University

Research Article

Keywords: GCM selection, Northern Nigeria, Climate change, Downscaling GCMs, CMIP6

Posted Date: August 31st, 2022

DOI: https://doi.org/10.21203/rs.3.rs-2002273/v1

Additional Declarations: No competing interests reported.

Version of Record: A version of this preprint was published at Theoretical and Applied Climatology on June 17th, 2023. See the published version at https://doi.org/10.1007/s00704-023-04534-w.

Abstract

Using multiple General Circulation Models (GCMs) for impact assessment improves the credibility of an analysis and circumvents limit-based uncertainties. Therefore, the selection of the most suitable models for regional/local studies is crucial prior to impact studies and forcing hydrological models. This study included the selection of GCM models from 100 ensembles each for SSP4.5 and SSP8.5 scenarios from the CMIP6 archive using advanced envelop-based selection approach for Northern Nigeria. We used (2021-2050) as the short-term and (2051-2080) as the long-term periods. The approach found that, CanESM5 models are skilful in simulating the warm and wet season, HadGEM3-GC31-LL in the warm and dry season, whereas MPI-ESM1-2-HR and MPI-ESM1-2-LR are skilful in the cold and dry season. We selected three skilled models for each scenario and study period. The skilled models were downscaled for adequate futuristic representation of the temperature and precipitation variables in the region. The downscaled variables predicted an increase in the future. Considering SSP4.5, the average annual precipitation predicted a 13% and 20% increase for the short-term and long-term period respectively. Similarly, for SSP8.5, the predictions are 23% and 41% increment in short-term and long-term periods respectively. For temperature, considering SSP4.5, the average annual temperature predicted an increase of 1.1 C and 2.5 C for short-term and long-term respectively. Similarly, an increment of 1.2 C and 2.7 C is expected for SSP8.5 during the short-term and long-term respectively. The selection also suggests that the skilled model does not vary with climate scenario and future periods.

Introduction

Scientific research concerning climate change has gain global attention in recent decades. Studies on future impact of climate change on the environment and water resources is essential for proper management and planning of large catchment. As noted by (Kim et al., 2011), Clausius-Clapeyron's theory reveals that climate change will alter hydrological processes bringing about the likelihood of more frequent extreme events. Likewise, changes in precipitation and modification of hydrological process will in return influence agricultural production, water resources and eco-hydrological systems (Li et al., 2009). However, in sub-Saharan Africa, few researchers have assessed the future impact of climate change on the environment and available water resources (Jin et al., 2018). In Nigeria, climate change studies are very few due to data scarcity, poor data collection, inaccessibility of data and deteriorated weather and hydrological stations. All these have been the barrier to accomplishing simulation of hydrological regime in the entire river basins in the country (Aladejana et al., 2018; Umar et al., 2018). The Hadejia, Jama'are, Sokoto Rima, Upper and Lower Benue, and Upper and Lower Niger River Basins Authorities are the major river basins in Northern Nigeria. These basins are tapped for urban and rural water supply, industrial and agricultural purposes. In recent times, the basins have undergone extreme hydrological changes leading to severe floods, droughts and other hydrological catastrophes. Several studies revealed that the basins are vulnerable to climate change (Adakayi, 2012; Sawa et al., 2015). It is therefore imperative to conduct GCMs appraisal prior to impact studies to understand the likeliness that it will influence the hydrological regime of the region including quantity of fresh water, surface runoff, soil erosion processes and precipitation pattern. On the other hand, agricultural water demands, rural, urban, and industrial water supply are on the rise due to rapid population increase in the region. Thus, addressing this problem in connection with climate change variability and its impact for sustainable water resources management requires a thorough understanding of the eco-hydrological system management based on predicted climate (Li et al., 2016).

Climate change impact studies are nearly impossible without the projection of future climate outputs from climate models (Lutz et al., 2016). The General Circulation Models (GCMs) simulates numerous atmospheric properties thereby representing a wide range of climatic processes at global scales. These climate processes are used for analyses such as future climate dynamics and changes in precipitation and temperature patterns. Despite having numerous GCMs, the number of these climate models keep increasing. Large number of GCMs outputs are used in the Intergovernmental Panel on Climate Change (IPCC) fourth, fifth, and sixth assessment reports. The Couple Model Intercomparison Project Phase 3 (CMIP3) archive (Meehl et al., 2007) contains different model output from 25 GCMs, while 61 different GCMs are present in the CMIP5 archive (Taylor et al., 2012), whereas, CMIP6 archive (Eyring et al., 2016) contains more than 100 GCMs output. GCMs models included in the CMIP often have multiple ensemble members, yielding an increasing number of model runs.

There has been improvement over time in GCMs models projections. CMIP6 models output have better representation in physical processes and spatial resolution and addresses various scientific gaps contained in previous CMIP. A major improvement include; uncertainties in scenarios and earth system response to forcing (Eyring et al., 2016). Despite these improvements, uncertainties still remain large and even increases with an increase in number of models available (Lutz et al., 2016). In view of the large number of climate models and computational constraints, the utilization of climate models for impact studies is only limited to few models. However, many models/ensembles have a poor representation of spatial and temporal climate pattern of a region (Kaini et al., 2020). Hence they cannot perfectly simulate past and future climatic characteristics of a local climate (Lee et al., 2019). Therefore, the selection of the best GCM output having the ability to represent past and future climatic characteristics for a specific region is an important task before conducting climate change impact assessment. It is important to note that, a single GCM cannot adequately represent the extreme of local climatic characteristics. (Kaini et al., 2020). Most often, multi-model ensemble mean demonstrate better capabilities to represent characteristics of local climate for impact study. Despite the importance, the

selection of the best models capable of simulating local climate is not straightforward and usually involves multiple criteria (Lutz et al., 2016). Which are:

1. Averaging some or all models with available data (e.g. Maghsood et al., 2019; Pierce et al., 2009; Seager et al., 2007; Zhang et al., 2019). The major setback of this method is equal weighting of good performing and poor performing GCMs (Pierce et al., 2009).
2. Using past performance approach by considering the ability of GCMs to simulate the past and present observed data (e.g Biemans et al., 2013; Pierce et al., 2009). In this method, there's the possibility of a model to perform well in simulating past climate but fail in representing the future climate equally well (Lutz et al., 2016).
3. The envelop approach, whereby GCMs are selected considering climatological variable of interest, such as mean air temperature, and annual precipitation among others (e.g Sorg et al., 2014; Warszawski et al., 2014). The major setback of this approach is that it only considers changes in annual means, also, model skill in simulating past climate are not considered, this gives rise to equal plausibility for all participating models (Lutz et al., 2016).

Lutz et al. (2016) recently developed a new method for the selection of representative climate models for the region of interest by combining the envelop approach and the past performance approach. The approach made emphasis in determining skilled GCMs for representing important climate futures such as means of temperature, annual precipitation, climate extreme, and past performance skills with respect to a reference climate data. Models that perform better in simulating past and present climate fluxes are usually selected for impact studies. The combined envelop and past performance approach still have some level of uncertainties. These uncertainties are related to the future pathway, as level of emitted gases, such as Green House Gases (GHG) in the future pathway remains uncertain (Ometto et al., 2014).

The grids size of GCM output are often coarse, their spatial resolution ranges from 100-500km grid size with temporal resolution of daily, monthly or even higher. Hence, forcing hydrological models or conducting impact studies using raw GCMs data is often not possible due to their coarse spatial resolution (Zollo et al., 2015). Hydrological simulation and climate change impact studies requires GCMs data at a fine spatial resolution. However, for suitability in climate change studies, GCMs are downscaled to finer resolution lower than 100km grid size using either statistical downscaling or through dynamic downscaling via Regional Climate Models (RCM). The downscaled output is then used to force hydrological models for impact assessment. Consequently, policy makers for climate change adaptation strategies and regulations use these assessments.

An observed or reference dataset is necessary for adequate evaluation of GCM models in the advanced envelope approach, and the study area is dearth of observed data. In recent studies, reanalysis models were found to be skilful in substituting observed datasets in a data scarce area. Multiple reanalysis models can be evaluated using Taylor diagram to obtain a skilled model for impact studies. Taylor diagram is a useful tool in evaluating the performance of climate models with respect to a reference dataset using the principle of cosine. Over the years, numerous intercomparison studies have applied the two dimensional diagram for evaluating scalar quantities such as temperature and precipitation (Jiang et al., 2015; Katragkou et al., 2015). The statistical matrices used for pattern comparison between observed and simulated in the Taylor diagram include the Pearson coefficient of correlation (CC), standard deviation (SD), and centred root-mean-squared error (RMSE). The CC measures the degree of phase agreement while the RMSE measures the agreement in amplitude of two fields. For a perfect simulation, RMSE would be equal to zero, and both CC and SD approaches one.

Previous studies conducted on climate change projection in Nigeria are based on few model runs and involve either statistical analysis, machine learning, or random selection of GCMs. Shiru et al. (2020a; 2020b) used gain ratio, entropy gain and symmetrical uncertainty machine learning processes to project the temperature and rainfall for Nigeria using CMIP5 models on different RCP scenarios. The study was conducted with twenty GCMs and Climate Research Unit (CRU) dataset as reference data. The analysis reveals that HadGEM2-ES, CESM1-CAM5, CSIRO-MK3-6-0, and MRI-CGCM3 have better skills in replicating temperature and rainfall characteristics in Nigeria. Other studies, Ndulue and Mbajiorgu (2019) randomly selected CSIRO-MK3-6-0 model to predict the impact of climate change on sediment and land use change on streamflow in an agricultural watershed in Upper Ebonyi River in Nigeria. Amodu and Ejieji (2017) evaluated twenty GCMs in the CMIP3 archive using observed data from Kano, Katsina, Sokoto, and Maiduguri States in Nigeria. They evaluated the GCMs by comparing the monthly values of temperature and precipitation in the sudan-sahel region of Nigeria using coefficient of correlation (r), mean absolute error (MAE), and root mean square error (RMSE) as metrics for the ranking of the most suitable GCMs. From the previous studies, none used the CMIP6 GCM output and the modified global warming scenarios. Furthermore, the studies did not consider climate extremes and past performance skills in simulating temperature and rainfall characteristics. In addition, only single model run was used, as multi-model runs exist for many GCMs. Finally, Nigeria consist of different climatic zones, averaging the predictability of seasonal, annual, and decadal climate behaviour of the entire country yields inadequacies in climate data prediction (Lutz et al., 2016).

Here, we used gridded dataset in a data scarce homogenous northern Nigeria region to determine the appropriate GCM output that have good skill in representing the temperature and rainfall characteristics as well as climate extremes using different global warming scenarios in short-term and long-term periods of the study area. Such analysis provides a better understanding in selecting GCMs for impact studies on the

hydrological regime. The main aim of this paper is to: (a) To evaluate reanalysis models that can substitute the observed dataset, (b) Select representative GCMs for the study area, and (c) develop high-resolution downscaled GCM output for the study area. We first evaluate reanalysis models and determine the best reanalysis model that can substitute observed dataset in the data scarce region. Then, with respect to the reference dataset, we selected skilled CMIP6 GCMs from pool of 100 model runs each of SSp4.5 and SSP8.5, which is the novelty of this research. Finally, we present the downscaled GCMs representing the study area for the two future periods. The study addresses the dearth in research findings due to poor observed data and provides insight in conducting impact studies.

2.1 Study Area and Data Description

The study is illustrated for an area comprising of Sokoto-Rima, Hadejia_Jama'are, Lower and Upper Niger, Lower and Upper Benue, River Basins (Figure 1). The area constitutes the two largest rivers in Nigeria (River Niger and Benue), and it is regarded as the agricultural hub of the country with catchment area of about 606,335Km^2. While evidence of climate change is pronounced in the region, there is scarcity of climate change research articles for the basins. More than 120 million people are utilizing the available water resources for agriculture, industrial, and domestic purposes. The result of this study will be vital in assessing future changes in climate and for forcing hydrological models for optimal management of water resources.

Historical reference datasets are necessary for the evaluation of GCM models in simulating the daily, monthly and annual cycle of air temperature and precipitation. We used three reanalysis datasets: NCEP/NCAR Reanalysis 1 (NCEP-1, Kalnay et al., 1996), NCEP-DOE Reanalysis 2 (NCEP-DOE, Kanamitsu et al., 2002), and ERA-5 (Hersbach et al., 2020; Hersbach & Dee, 2016). The reanalysis datasets were evaluated with observed data using Tailor diagram (Taylor, 2001) from 1981-2010 after remapping to a common grid.

A number of radiative forcing scenarios drive the CMIP6 climate models from multiple socioeconomic assumption in the form of "Shared Socioeconomic Pathways" (SSPs) (O'Neill et al., 2016). For this study, we selected a set of tier 1 scenarios to provide a range of projection towards the end-of-century. Two radiative forcing levels adopted are the "middle of the road" (SSP2-4.5) and "worst case scenario" (SSP5-8.5) referred herein as SSP4.5 and SSP8.5, respectively. As a criterion for model selection, models run must have output data from the paired forcing, and having daily and monthly data values extending to 2100. These criteria yielded a pool of 200 (100 ensemble each for SSP4.5 and 8.5) models runs from 20 GCMs and were categorised as short-term (2021-2050) and long-term (2051-2080) periods. We downloaded climate models from the World Climate Research programme (WCRP) database at (https://esgf-node.llnl.gov/projects/cmip6/) in September 2020. We processed the climate data and calculate climate extremes as defined by the Expert Team on Climate Change Detection and Indices (ETCCDI) using the Climate Data Operators (CDO-version 1.9.9), developed by the Max Planck Institute for Meteorology (Schulzweida, 2020). Climate Data Operators (CDO) is a collection of command line operators for analysing and processing climate models data. It has more than 600 operators available and support GRIB1/2, netCDF3/4, IEG, EXTRA, and SERVICE data formats.

Methods

3.1 Evaluation of reference data set

Taylor diagram (Taylor, 2001) shows how well pattern resembles between simulated and observed climate variables. The correlation coefficient (CC), centred root-mean-square error (RMSE), and the standard deviation (SD) are the statistical metrics used for evaluation in the Taylor diagram. In-depth information on Taylor diagram is described in (Taylor, 2001; Taylor, 2005). We selected reanalysis models with available daily and monthly output for the study area. The temperature and precipitation variables of NCEP-DOE, ERA5, and NCEP-1 reanalysis models were evaluated using observed data from the Nigerian meteorological Agency (NiMet). NiMet stations are dispersed, and are placed at more than 50km apart. Six stations (Kano, Sokoto, Bauchi, Kaduna, Niger, and Benue) were used for the evaluation of the reanalysis datasets for the studied period (1981–2010). This method has been widely used to evaluate the performance of reanalysis datasets and are found to give useful results (Koutsouris et al., 2016; Li et al., 2021; Rapaić et al., 2015; Tang et al., 2020). To measure the pattern of correspondence, the reanalysis datasets were interpolated to a common grid resolution of (0.5°×0.5°) and are average over the study area before plotting on the two-dimensional Taylor diagram plot using R package (R-Taylor diagram). The reference point on the plot both have CC and SD equal to one.

3.2 GCM selection method

Numerous climate models are continually participating in the Couple Model Intercomparison Project phase 6 (CMIP6) leading to a wide spectrum of the models. Substantial number of climate models runs exist, leaving the modeller in search of the so-called "best model". A comprehensive evaluation of these GCMs is essential for proper representation in impact studies. Normally, the determination of representative GCM of a specific area is done by utilizing various techniques dependent on a solitary or set of numerous rules. The present study adopted an advanced envelop based criteria developed by (Lutz et al., 2016). This approach involves a step-wise procedure in selecting GCMs based on the range of projected average annual changes of (a) mean temperature and precipitation sum, (b) climate extremes of temperature and precipitation, with respect to a reference period, and (c) refinement based on the model skill in producing the past climate. The intention of these

processes was to limit the number of climate models that can suitably represent a region of interest when conducting a climate change analyses. This method was applied to select a representative climate model for SSP4.5 and SSP8.5 during short term (2021–2050) and long-term (2051–2080) periods.

3.2.1 Initial selection process (step 1): Changes based on climate means

The initial selection is established based on the range of projected annual changes in the mean air temperature (ΔT) and precipitation sum (ΔP) using 1981–2010 reference period, 2021–2050 short-term period, and 2051–2080 long-term period averaged over the 1.0 × 1.0 grid cell of the study area (Fig. 1). The data were analysed and processed using CDO.

The process began by downloading monthly values of air temperature and precipitation time series for the observed (reference) period and the projected period of each year as mentioned in section 2.1. Subsequently, the area-average monthly air temperature and precipitation sum were computed for both periods. Furthermore, the annual mean air temperature and annual total precipitation for each year during the historical and future periods were determined and the ranges of changes in annual mean air temperature ΔT (C) and annual precipitation ΔP (%) was calculated using the reference period. Ultimately, the 10th and 90th percentile values for ΔT and ΔP were calculated for the reference and all model runs after remapping GCMs and reference data to a common grid of 1.0 × 1.0 .

Extreme climate does not exist in the study region, rather than using much lower and higher percentile values representing the distinct seasons, the 10th and 90th percentile values were considered based on the nature of the climate in the concerned region. The 10th and 90th percentile of the reference period represents the focal point of the spectrum of projection for changes in temperature and precipitation. Four distinct seasons are normally experienced in the region namely; cold and dry, hot and dry, warm and wet, and warm and dry (Tanko & Momale, 2013). This study considers three (3) spectra for the analysis. The proximity of all the model runs from each corner of the spectrum with respect to their projection was calculated using Eq. 1 viz:

$$D_{p_j^P, p_j^T} = \sqrt{\left(P_i^P - P_j^P\right)^2 + \left(P_i^T - P_j^T\right)^2}$$

1

Where $D_{p_j^P, p_j^T}$ is the proximity of a model to the corner under consideration, (j)'s ΔT (C) and ΔP (%) (P_j^T and $P_j^P \text{respectively}$) are the delta changes of each model ensemble, and (i)'s ΔT and ΔP (P_i^T and P_i^P respectively) are the 10th and/or 90th percentile score for each ensemble. Finally, five models with the closest proximity to each corner of the spectrum were selected and ranked, making fifteen model runs for each SSP.

3.2.2 Refined process (step 2): Changes based on climate extremes

In this step, the fifteen models selected during the selection process where further refined based on their projected changes in climate extremes. Climate indices from the Expert Team on Climate Change Detection and Indices (ETCCDI) (Peterson, 2005) were used to evaluate projected changes in climate extremes with respect to the reference period. As the product of this research will be used to simulate hydrological and crop growth models for impact assessment, emphasis was made on two ETCCDI indices each for both air temperature and precipitation (Table 1) which are important in the entire study area. For evaluation of air temperature extreme, the warm spell duration index (WSDI) and cold spell duration index (CSDI) are considered. However, for the calculation of precipitation extreme, the number of consecutive dry days (CDD) and the precipitation due to extremely wet days (R95pTOT) are considered. The calculation of the ETCCDI indices were done using the CDO software from the daily model output of reference period (1981–2010) and future period (2021–2050) and (2051–2080) for short-term and long-term periods respectively. The indices were first calculated on their original grid before re-gridding to a common grid size and unit over the entire study area (Fig. 1). The indices are averaged over a 30-year period for both the future period and the reference period. Subsequently, the changes in CSDI, WSDI, R95pTOT, and CDD were calculated as percentual change of the projected period with respect to the reference period. After the calculation, the combination of two indices corresponding to each corner of the spectrum were selected. Such that WSDI and CDD represent the warm and wet corner, CSDI and CDD represent the cold and dry corner, while the combination of WSDI and R95pTOT represent the warm and wet corner. A ranking methodology was adopted from Lutz et al. (2016) such that temperature and precipitation for each model run were scored T-index and P-index rank, respectively based on the percentual increase of relevant indices. The model with the highest rank increase score five point, while the lowest increase score one point for that index. A combine score was obtained after averaging T-index and P-index. Finally, two model runs with the largest combined score at each corner are selected and qualify for the next step.

Table 1
Definitions of the ETCCDI indices governing the refined process (step 2)

Climate variable	ETCCDI index	Index definition
Precipitation	R95pTOT	Annual total precipitation when RR > 95 percentile. Let RR_{wj} be the daily precipitation amount on a wet day (w) (RR ≥ 1.0mm) in period i and let $RR_{wn}95$ be the 95th percentile of precipitation on wet days, then $R95p_j = \sum_{w=1}^{W} RR_{wj} \text{ where } RR_{wj} > RR_{wn}95$
Precipitation	CDD	Consecutive dry days: Maximum length of dry spell with RR < 1mm: Let RR_{ij} be the daily precipitation amount on day i in period j. Count the largest number of consecutive days where: RR_{ij} < 1mm
Temperature	WSDI	Warm spell duration index: Annual count of days with at least 6 consecutive days when TX > 90th percentile (TX_{ij} is the daily T_{max} on day i in period j)
Temperature	CSDI	Cold speel duration index: Annual count of days with at least 6 consecutive days when TN < 10th percentile (TN_{ij} is the daily T_{min} on day i in period j

3.2.3 Final process (step 3): Selection based on past performance skill

The remaining models are further evaluated based on their skill in simulating the past climate. Taking into consideration all monthly values of the model runs spanning through the 30 years of the reference period (1981–2010). The study area in this step is subdivided into three subdomain viz: Upper and Lower Niger (ULN), Upper and Lower Benue (ULB), and Sokoto-Hadejia_Jama'are (SHJ) to enable proper validation with respect to the reference dataset. The analysis is done per subdomain to capture areas with similar temperature and precipitation pattern on the entire domain. This analysis is necessary to avoid underestimation or overestimation in the study area (Lutz et al., 2016). The models in this step are assessed based on their ability to simulate the reference dataset for monthly average mean temperature and monthly precipitation. If a model simulates the reference data accurately, the skill score approaches one. The calculation of skill score for temperature and precipitation are different. For calculating and assessing the performance of each model in simulating past temperature, we adopted a method developed by Perkins et al. (2007). We measured the common area between two probability density functions (PDFs) by calculating the cumulative minimum distribution value of two binned values viz:

$$S_{score} = \sum_{1}^{n} minimum\left(Z_{GCM} Z_{ref}\right) \quad (1)$$

Where n is the number of bin used to calculate the PDF, Z_{GCM} is the frequency of values in a given bin from the GCM, and Z_{ref} is the frequency of values from the reference data, we used 100 bins for the analysis.

for precipitation, the approach of Sanchez et al. (2009) is used. The procedure consists of a collection of five equations as a product of skill score function. Each of the function assess similarities between the observed and the modelled data, while considering different behaviour of precipitation. This skill scores equation are listed here viz;

$$f_1 = 1 - \left(\frac{|A_{GCM} - A_{NCEP-DOE}|}{2 \cdot A_{NCEP-DOE}}\right)^{0.5} \quad (2)$$

$$f_2 = 1 - \left(\frac{|A^{+}_{GCM} - A^{+}_{NCEP-DOE}|}{2 \cdot A^{+}_{NCEP-DOE}}\right)^{0.5} \quad (3)$$

$$f_3 = 1 - \left(\frac{|A^{-}_{GCM} - A^{-}_{NCEP-DOE}|}{2 \cdot A^{-}_{NCEP-DOE}}\right)^{0.5} \quad (4)$$

$$f_4 = 1 - \left(\frac{\left|\bar{P}_{GCM} - \bar{P}_{NCEP-DOE}\right|}{2 \cdot \bar{P}_{NCEP-DOE}}\right)^{0.5} \quad (5)$$

$$f_5 = 1 - \left(\frac{|\sigma_{GCM} - \sigma_{NCEP-DOE}|}{2 \cdot \sigma_{NCEP-DOE}} \right)^{0.5} \quad (6)$$

$$SKpre = f1.f2.f3.f4.f5 \, (7)$$

Where A_{GCM} and $A_{NCEP-DOE}$ denotes the areas below the cumulative distribution function (CDF) of the GCM and the reference model respectively, taking into account the distribution as a whole through the total area below the CDF (Eq. 2) and the mean (Eq. 5). Similarly, $A^{+}$and A^{-} (Eqs. 3 & 4) denotes the fractional areas right and left of the 50th percentile respectively, accounting for the high and low precipitation. P is the average annual precipitation over the entire study area. σ is the standard deviation of the CDF accounting for the shape of the distribution through the variance (Eq. 6). Multiplying the five skill scores equations for individual model yielded a total (SK_{pre}) skill score of precipitation (Eq. 7). The skill scores were calculated and assigned for temperature and precipitation for the individual subdomain separately. For each subdomain, we calculated the average of temperature and precipitation skill score and then ranked. Finally, the ranking is summed for each GCM model resulting in a final ranking of the entire study area.

3.3 Downscaling of climate models

GCMs output are coarse and biased with respect to observation and their projection have limited skill in resolving local climate. Due to this mismatching spatial resolution and biases, processing GCMs output is necessary before conducting impact studies. To overcome this problem, downscaling is introduced to obtain high-resolution climate data from low-resolution climate variables (Fowler et al., 2007). Two downscaling techniques exist: dynamical and statistical downscaling technique. The former uses GCMs output to drive Regional Climate Models (RCMs) to generate high-resolution climate variable for local climate analysis (Maraun et al., 2010). The later uses statistical means to establish relationship between local observation variables and GCMs output at a specific location (Fowler et al., 2007). RCMs has no stationarity in projecting future projections but are computationally expensive and time consuming. For a robust local impact studies, RCM output needs to be bias-corrected (Gudmundsson et al., 2012; Piani et al., 2009). Statistically downscaled variables are computationally efficient and multiple GCMs and scenarios can run in a limited amount of time but the output have stationarity problem in projecting future dynamics. Most importantly, this method automatically correct the biases in GCM output and provide climate variables at point-scale (Fowler et al., 2007).

After the final selection of the GCMs, we selected three statistical methods to downscale the coarse GCMs using 17 strategic stations on the study region for proper representation in hydrological models. The techniques include: (1) Delta change (DC) (2) Quantile Mapping (QM) and (3) Empirical Quantile Mapping (EQM). For more information about these approaches refer to (Chen et al., 2012; Hertig & Jacobeit, 2008; Maraun, 2013; Räty et al., 2014; Wilby et al., 2002). Statistical techniques for downscaling GCM varies in their output, hence results in different strengths and weakness (Werner & Cannon, 2016). For the temperature and precipitation variables, the selection of suitable downscaling technique was made after evaluating their performance using the following statistical test: (1) Root Mean Square Error (RMSE); (2) Nash Sutcliffe efficiency coefficient (NSE); (3) Mean Absolute Error (MAE); (4) Pearson Correlation, (5) Spearman correlation and (6) Index of Agreement with respect to the reference data set. Using multiple techniques for statistical downscaling provide insight in obtaining the best relationship between modelled and observed variable.

Results And Discussion

The results obtained are demonstrated and discussed in the following subsections.

4.1 Selection of reference data

Based on the output from the Taylor diagram, the precipitation and temperature variables of NCEP-DOE reanalyses model has the highest correlation coefficient (CC) with values of 0.774 and 0.783 respectively compared to ERA5 and NCEP1 models (Table 2). The ration of the standard deviation (SD) of the reanalyses models to the observed dataset gave a good performance for NCEP-DOE reanalyses model. The ratio of the precipitation and the temperature is 0.686 and 0.72 respectively. The NCEP-DOE model performs better than the other models based on the performance indices as shown in Figure 3.

Table 2 Values of correlation coefficient of reanalysis models relative to observation

VARIABLE	MODEL	RATIO	CORRELATION OF COEFFICIENT
Precipitation	ERA-5	0.491	0.773
	NCEP-DOE	0.686	0.774
	NCEP1	0.699	0.701
Temperature	ERA-5	0.619	0.584
	NCEP-DOE	0.72	0.783
	NCEP1	0.697	0.623

Having a good performance, NCEP DOE reanalysis model has never been evaluated in the study region but has been applied around the world including sub-Saharan Africa where the study area lies (Zhan et al., 2016). Some reanalysis models have been used in Nigeria such as the Global Precipitation Climatology Centre (GPCC-V6) and Climatic Research Unit (CRU - version TS v. 3.23) (Shiru et al., 2021). However, the precipitation variable of the GPCC, the University of Delaware (UDEL) and NOAA's Gridded Precipitation Reconstruction Over Land (PREC/L) have poor performance in the Northern part of Nigeria during the dry season but performed better during the wet season (Ogunjo et al., 2022).

4.2 Selection of representative GCM

4.2.1 Changes based on climate means

Changes in projected annual mean air temperature (ΔT) and annual precipitation (ΔP) for the short-term and long-term period with respect to the reference period are the bases for the initial selection process. We selected the five models closest to the 10th and 90th percentile value of temperature and precipitation representing cold and dry, hot and dry, and hot and wet corner (Figure 2). Some models show a close proximity and cluster around the vicinity of the respective corners, while others show a larger proximity and scatter around a corner. For example, the warm and dry corner for SSP4.5 and SSP8.5 during the short-term period, and the warm and dry, and warm and wet corner of SSP8.5 during the long-term period (Figure 2A, 2C and 2D) showed a close proximity. However, the cold and dry corner of SSP8.5 during the short-term and long-term period showed a scattered and a distant proximity to the corner. Interestingly, all CanESM5 models aligned towards the warm and wet corners for all study periods, all FGOALS-g3 and HadGEM3-GC31_LL ensembles aligned towards the warm and dry corner for all period except SSP8.5 during the long-term period where UKESM1-0 replaces FGOALs-g3. Majority of MPI-ESM1-2-LR ensembles occupies the cold and dry corner for all periods.

Values from the five models selected from each corner yielded a range of changes from the reference data set. The ΔT and ΔP range of projection for SSP8.5 are higher than SSP4.5 during the same period. The projection for ΔT and ΔP during the short-term ranges from 0.1-2.7 C and -2.6–4.4% respectively for SSP4.5 (Figure 2A), whereas for SSP8.5 (Figure 2C), the ranges are 0.1-3.5 C and -2.8-5.8% respectively. Likewise, the ranges of ΔT and ΔP during the long-term period are 0.3-2.8 C and -2.6-5.7% respectively for SSP4.5 (Figure 2B), whereas for SSP8.5 (Figure 2D), the ranges are 0.4-4.5 C and -1.3-7.7% respectively. Similarly, the ranges of projection for ΔT and ΔP is much higher for the long-term period compared to the short-term period during the same forcing pathway. Considering SSP4.5 (Figure 2A), the ΔT and ΔP ranges are 0.1-2.7 C and -2.6-4.4%, respectively, during the short-term period, whereas the ranges are 0.3-2.8 C and -2.6-5.7%, respectively, during the long-term period (Figure 2B). Likewise, considering SSP8.5, the ranges are 0.1-3.5 C and -2.8-5.8% during the short-term period (Figure 2C), whereas the ranges are 0.4-4.5 C and -1.3-7.7% during the long-term period (Figure 2D), respectively. This step leads the selection approach; this may result in reducing a substantial number of models for subsequent steps. The non-selected models might have good skills in simulating the climate extreme or the past climate. Another issue is the fact that the projected changes are averaged over the study area, which may result in dilution of spatial variation in projected changes. However most studies covering large areas exhibit similar methodology (Lutz et al., 2016).

4.2.2 Changes based on climate extremes

The models selected from the initial selection process (step 1) were subjected to changes in two ETCCDI indices for both temperature and precipitation for short-term period (2021-2050), long-term period (2051-2080) and the reference period (1981-2010). In this process, two models runs having highest combined scores from the combined temperature and precipitation indices were selected from each corner. In the event that multiple models runs have the same second highest combined score, more than two models are selected for that corner (Table 3). It is observed that, when computing combine score, some models with highest value change in one ETCCDI indices are not selected as a result of having a lower change in another ETCCDI indices. For example, in the warm and wet corner of SSP8.5, for the long-term period, the model CanESM5_r4i1p1f1 projects the highest change in R95pTOT, however, CanESM5_r6i1p1f1 and CanESM5_r9i1p1f1 were selected instead, due to its lower combined score. From (Table 3), models projecting large changes in mean air temperature results in projecting large changes in WSDI indices. Similarly, large changes in precipitation sum also project large changes in R95pTOT. For example, for SSP4.5, FGOALS-g3_r2i1p1f1 projected the largest increase in mean air temperature likewise show the largest increase in WSDI. Moreover, HadGEM3-GC31-LL_r1i1p1f2

shows a good combined score and present in all the warm and dry corner of the entire study period for both SSP4.5 and SSP8.5. Considering all the models relative to the corner and the season they appear, CDD is expected to decrease up to 112.7% in short-term, 113% in the long-term considering SSp4.5. Likewise, CDD is also expected to decrease up to 110.9% in short-term, 116.5% in long-term period considering SSP8.5. In addition, R95pTOT shows an increasing trend up to 137.8% in short-term, 139.1% in long-term considering SSP4.5. Similarly, R95pTOT increase up to 168.7% in short-term, 212.6% in long-term considering SSP8.5. Decrease in CDD and an Increase in R95pTOT predicts more wet days during rainfall seasons. The WSDI is projected to increase up to 3758.9% in short-term, 4159.0% in long-term considering SSP4.5. Likewise, WSDI is projected to increase by 4175.1% in short-term, 4692.3% in long-term considering SSP8.5. The CSDI is projected to decrease for all the study periods with the exception of EC-Earth-Veg_r1i1p1f1 which shows an increase of 9% with respect to the reference period. Increase in WSDI indicates an increase in maximum temperature, while a decrease in CSDI implies warm nights are expected in the future periods. Similar to step 1, area-averaged was applied to this step. This problem can be solved by dividing the area into homogenous entities.

Table 3 GCMs selected based on changes in ETCCDI indices. Model runs selected for step 3 are coloured with yellow

Seasonal projection	GCM Model Runs	ΔCDD(%)	Δr95ptot(%)	ΔWSDI(%)	ΔCSDI(%)	ΔT(°C)	ΔP(%)	T Index rank	P index rank	Average Score
		SSP4.5 (2021-2050)								
	FGOALS-g3_r1i1p1f1	-17.7	55.9	5149.8	-99.9	2.6	-2.3	3	4	3.5
	FGOALS-g3_r2i1p1f1	-22.8	56.3	5228.9	-99.5	2.8	-2.2	5	1	3
warm and dry	FGOALS-g3_r3i1p1f1	-21.3	55.2	5191.2	-98.5	2.7	-2.3	4	2	3
	FGOALS-g3_r4i1p1f1	-19.5	58.7	5121.5	-99.9	2.7	-2.7	1	3	2
	HadGEM3-GC31-LL_r1i1p1f3	-14.4	53.2	5135.7	-13.8	2.1	-1.7	2	5	3.5
	MIROC-ES2L_r1i1p1f2	-30.3	65.5	5284.6	-100.0	2.5	4.4	5	1	3
	CanESM5_r5i1p1f1	-16.1	68.1	3751.4	-92.7	1.9	4.3	4	4	4
warm and wet	CanESM5_r7i1p1f1	-12.1	69.9	3711.4	-98.0	1.9	4.2	3	5	4
	CanESM5_r10i1p1f1	-13.8	67.8	3554.7	-90.8	1.8	4.3	1	3	2
	CanESM5_r22i1p1f1	-10.0	66.6	3673.6	-85.6	1.8	4.3	2	2	2
	INM-CM4-8_r1i1p1f1	-24.0	-13.7	713.2	-91.3	0.1	-1.9	1	1	1
	MPI-ESM1-2-LR_r6i1p1f1	0.8	-47.5	2460.2	-83.9	0.7	-1.9	3	4	3.5
cold and dry	CNRM-CM6-1_r1i1p1f2	1.7	30.4	2535.3	-65.4	0.4	-1.6	5	5	5
	MPI-ESM1-2-LR_r3i1p1f1	-0.2	-44.1	2520.2	-89.5	0.7	-1.8	2	2	2
	MPI-ESM1-2-LR_r5i1p1f1	0.6	-45.3	2398.5	-78.6	0.6	-1.7	4	3	3.5

SSP8.5 (2021-2050)

	FGOALS-g3_r3i1p1f1	-19.5	58.6	5139.7	-100.0	3.2	-2.3	1	2	1.5
	FGOALS-g3_r4i1p1f1	-17.9	60.4	5234.2	-99.2	3.3	-2.6	3	4	3.5
warm and dry	FGOALS-g3_r1i1p1f1	-18.0	60.9	5224.5	-99.8	3.2	-2.6	2	3	2.5
	HadGEM3-GC31-LL_r1i1p1f3	-16.7	60.9	5792.8	-47.5	3.5	-1.9	5	5	5
	FGOALS-g3_r2i1p1f1	-19.8	59.1	5236.4	-99.6	3.3	-2.8	4	1	2.5
	CanESM5_r24i1p1f1	-10.7	69.0	3759.8	-90.6	2.9	5.4	2	3	2.5
	CanESM5_r12i1p2f1	-13.0	65.9	3171.8	-97.8	2.9	5.4	1	2	1.5
warm and wet	CanESM5_r3i1p1f1	-9.7	71.3	3903.5	-92.7	2.8	5.6	5	4	4.5
	CanESM5_r11i1p1f1	-11.9	65.7	3887.6	-86.1	2.9	5.8	4	1	2.5
	CanESM5_r16i1p1f1	-14.6	79.0	3783.7	-90.5	2.8	5.5	3	5	4
	CNRM-CM6-1_r1i1p1f2	-4.2	36.1	2499.6	-68.3	1.7	-2.3	4	2	3
	EC-Earth3-Veg_r1i1p1f1	23.7	-23.2	2237.3	193.8	0.1	-1.9	5	5	5
cold and dry	MPI-ESM1-2-LR_r5i1p1f1	0.1	-39.1	2038.6	-85.9	1.4	-1.5	2	3	2.5
	MPI-ESM1-2-LR_r9i1p1f1	1.4	-40.6	2088.9	-75.7	1.3	-1.5	3	4	3.5
	INM-CM4-8_r1i1p1f1	-20.6	-19.5	1071.1	-95.2	0.6	-1.4	1	1	1

SSP4.5 (2051-2080)

	FGOALS-g3_r3i1p1f1	-23.8	60.0	5598.1	-99.9	2.7	-2.4	1	1	1
	FGOALS-g3_r4i1p1f1	-19.3	60.9	5688.0	-99.9	2.7	-2.4	2	2	2
warm and dry	FGOALS-g3_r2i1p1f1	-16.1	61.2	5714.0	-100.0	2.8	-2.6	4	4	4
	FGOALS-g3_r1i1p1f1	-19.1	60.0	5688.7	-100.0	2.8	-2.6	3	3	3
	HadGEM3-GC31-LL_r1i1p1f3	-14.6	52.3	5771.0	-80.6	2.3	-1.1	5	5	5
	CanESM5_r3i1p1f1	-11.0	70.3	4957.3	-95.1	2.0	5.5	1	5	3
	CanESM5_r6i1p2f1	-13.0	62.4	5086.6	-97.5	2.1	5.1	5	1	3
warm and wet	CanESM5_r8i1p1f1	-13.9	68.5	4966.2	-94.0	2.0	5.4	2	2	2
	CanESM5_r9i1p1f1	-13.0	69.4	5065.1	-99.0	2.0	5.7	4	3	3.5
	CanESM5_r1i1p1f1	-12.3	69.8	4978.1	-96.8	1.9	5.6	3	4	3.5
	INM-CM4-8_r1i1p1f1	-24.6	-5.0	1383.0	-99.1	0.3	-2.0	1	1	1
	CNRM-CM6-1_r1i1p1f2	-1.3	22.8	4396.9	-97.1	0.4	-1.4	4	3	3.5
cold and dry	MPI-ESM1-2-LR_r9i1p1f1	-2.2	-43.7	3678.9	-98.1	0.5	-1.4	3	2	2.5
	MPI-ESM1-2-LR_r3i1p1f1	1.0	-42.9	3776.2	-95.3	0.5	-1.4	5	4	4.5
	MPI-ESM1-2-LR_r10i1p1f1	2.7	-40.6	3724.9	-98.4	0.5	-1.3	2	5	3.5

SSP8.5 (2051-2080)

	HadGEM3-GC31-LL_r1i1p1f3	-14.0	61.4	6493.5	-95.0	4.5	-1.3	5	3	4
	UKESM1-0_r2i1p1f2	-19.9	63.6	6249.7	-84.8	4.1	-0.8	3	2	2.5
warm and dry	UKESM1-0_r3i1p1f2	-22.9	70.2	6328.3	-88.4	4.2	-0.7	4	1	2.5
	UKESM1-0_r8i1p1f2	-9.1	64.6	6055.0	-85.8	3.9	-0.7	1	5	3
	UKESM1-0_r1i1p1f2	-12.7	64.3	6223.0	-89.8	4.0	-0.6	2	4	3
	CanESM5_r22i1p1f1	-13.4	87.2	6414.8	-100.0	4.2	7.4	4	1	2.5
	CanESM5_r6i1p1f1	-11.4	89.2	6377.4	-97.2	4.1	7.5	3	4	3.5
warm and wet	CanESM5_r9i1p1f1	-10.4	87.5	6423.7	-100.0	4.2	7.2	5	3	4
	CanESM5_r12i1pf1	-11.4	87.2	6372.5	-100.0	4.0	7.4	2	1	1.5
	CanESM5_r4i1p1f1	-9.4	91.9	6315.1	-100.0	4.1	7.7	1	5	3
	INM-CM4-8_r1i1p1f1	-27.3	-2.0	2924.7	-99.5	1.5	-0.7	2	2	2
	INM-CM5-0_r1i1p1f1	-31.2	11.6	2868.8	-99.9	1.6	-0.7	1	1	1
cold and dry	MPI-ESM1-2-HR_r1i1p1f1	5.1	-13.4	5082.7	-97.8	2.2	-1.2	4	3	3.5
	MPI-ESM1-2-HR_r2i1p1f1	5.2	-5.2	5103.1	-98.3	2.1	-0.8	3	4	3.5
	EC-Earth3-Veg_r1i1p1f1	19.6	23.9	3542.9	-12.9	0.4	-0.4	5	5	5

4.2.3 Selection based on past performance skill

The models are subjected to a validation process based on their past performance skill in reproducing the NCEP-DOE reference dataset. Table 4 list the skill score for the GCM runs available after step 2. Table 5 list the combined score ranking for air temperature and precipitation resulting in the final ensemble selection (Table 6). From the precipitation and temperature skill score, it can be seen that the models that show good skill in simulating past climate for a particular subdomain, show equally a good skill in simulating the remaining subdomain. For example, HadGEM3-GC31-LL_r1i1p1f3, MPI-ESM1-2-LR_r9i1p1f1 and MPI-ESM1-2-LR_r10i1p1f1 exhibits good skill in all subdomain. Similarly, models with low skill for a particular subdomain show similar trend in another subdomain, for example CanESN5_r3i1p1f1.

CanESM5 model runs exhibit skill in capturing the warm and wet corner of the seasonal projection of the study area. The model however shows relatively good skill in simulating the past temperature for all subdomain but are poor in simulating past annual precipitation cycle in the entire subdomain. HadGem33-GC31_LL_r1i1p1f3, FGOALS, and UKESM1-0 models falls under the warm and dry corner. All the models show good skills in past performance for all subdomain. HadGEM3_GC3-1_LL_r1i1p1f3 show outstanding characteristics for both SSP4.5 and SSP8.5 and for all warm and dry corner by having a final skill score of 1. Similarly, MPI-ESM1-2-LR and MPI-ESM1-2-HR show good skill in representing both temperature and precipitation in the cold and dry corner.

Finally, Table 6 reveals that, the skilled GCM for a respective corner do not vary with radiative forcing scenarios (SSP4.5 and SSP8.5) as well as analysis period (short-term and long-term period), for example CanESM5 is selected in all warm and wet corner. However, the GCMs only exhibit different variant-ID in the CMIP6 metadata model runs, for example in the r1i1p1f1 nomenclature. The Realization (r) varies from r1-r10, with all Initialization (i) and Physics (p) as 1, and the Forcing (f) as 1 or 3 for all the model ensembles.

Table 4 Temperature and precipitation skill scores for the three subdomains

As stated earlier, some models with good skills in simulating the past climate might have been de-selected in the previous steps. Another limitation has to do with the final skill score calculation, which combines the precipitation and temperature skill scores.

The CMIP6 models have gained global applications for impact studies including Africa. However, the findings of the current study do not support a research conducted by Shiru et al. (2021) in Nigeria. They evaluated 13 historical GCMs each for minimum and maximum temperature and precipitation using only the first ensemble member (r1i1p1f1) of the models. Their ranking involve the application of compromise programming (CP) to rank the GCMs, while NRMSE, Pbias, NSE, R2 , and VE statistical performance measures were used for the evaluation. The concluded that, IPSL-CM6A-LR, NESM3, CMCC-CM2-SR5, and ACC-ESM1.5 have highest skills in simulating precipitation. For maximum temperature, the models INM-CM4-8, BCC-CSM2-MR, MRI-ESM2-0, and ACCESS-ESM1-5 performed better, while AWI-CM-1–1-MR, IPSL-CM6A-LR, INM-CM5-0, and CanESM5 are skilful in simulating the minimum temperature. Among these models, only CanESM5 was found to have good skills in this present study. A possible explanation for this result might be because of the different reference data sets used for

GCM runs	Precipitation Skill Score			Temperature Skill Score		
	ULN	ULB	SHJ	ULN	ULB	SHJ
CanESM5_r3i1p1f1	0.06	0.16	0.12	0.34	0.32	0.41
CanESM5_r5i1p1f1	0.07	0.27	0.15	0.47	0.44	0.49
CanEsm5_r6i1p1f1	0.05	0.16	0.09	0.39	0.33	0.28
CanESM5_r7i1p1f1	0.04	0.12	0.09	0.38	0.4	0.35
CanESM5_r9i1p1f1	0.08	0.23	0.14	0.42	0.49	0.45
CanESM5_r1i1p1f1	0.05	0.21	0.11	0.29	0.46	0.39
CanESM5_r16i1p1f1	0.06	0.15	0.11	0.27	0.35	0.38
CNRM-CM6-1_r1i1p1f2	0.27	0.27	0.25	0.43	0.44	0.42
HadGEM3-GC31-LL_r1i1p1f3	0.44	0.44	0.49	0.67	0.64	0.68
UKESM1-0-LL_r1i1p1f2	0.41	0.37	0.57	0.65	0.58	0.71
UKESM1-0-LL_r8i1p1f2	0.41	0.43	0.56	0.65	0.66	0.77
EC-Earth3-VEG_r1i1p1f1	0.11	0.1	0.09	0.36	0.33	0.29
FGOALS_g3_r1i1p1f1	0.36	0.13	0.25	0.34	0.27	0.41
FGOALS_g3_r2i1p1f1	0.28	0.08	0.22	0.29	0.22	0.33
FGOALS-g3_r4i1p1f1	0.3	0.05	0.16	0.2	0.19	0.29
MPI-ESM1-2-HR_r1i1p1f1	0.3	0.22	0.18	0.41	0.39	0.36
MPI-ESM1-2-HR_r2i1p1f1	0.3	0.22	0.17	0.44	0.41	0.4
MPI-ESM1-2-LR_r3i1p1f1	0.38	0.37	0.36	0.55	0.53	0.57
MPI_ESM1-LR_r5i1p1f1	0.23	0.22	0.18	0.56	0.51	0.47
MPI-ESM1-2-LR_r6i1p1f1	0.24	0.23	0.25	0.41	0.43	0.39
MPI-ESM1-LR_r10i1p1f1	0.41	0.41	0.33	0.67	0.69	0.59
MPI-ESM1-LR_r9i1p1f1	0.45	0.45	0.4	0.55	0.58	0.53

both studies. In addition, in their study, minimum and maximum temperature were used separately, while ours considers the mean temperature. Another possibility is the presence of heterogeneous climate in Nigeria, which our study considers by focusing in the Northern part of the country having homogenous climate.

Table 5 Final ranking of GCM runs for the three subdomains

Period	SSP	Seasonal Projection	GCM Runs	Average score per subdomain			Rank per subdomain			Total	Final rank
				ULN	ULB	SHJ	ULN	ULB	SHJ		
2021-2051	4.5	*Warm and Dry*	FGOALS_g3_r1i1p1f1	0.35	0.20	0.33	13	26	12	51	18
			HadGEM3-GC31-LL_r1i1p1f3	0.56	0.54	0.59	1	3	3	7	1
		Warm and Wet	CanESM5_r5i1p1f1	0.27	0.36	0.32	18	13	14	45	13
			CanESM5_r7i1p1f1	0.21	0.26	0.22	25	20	25	70	22
		Cold and Dry	CNRM-CM6-1_r1i1p1f2	0.35	0.36	0.34	13	13	10	36	11
			MPI_ESM1-2-LR_r5i1p1f1	0.40	0.37	0.33	10	10	13	33	10
			MPI-ESM1-2-LR_r6i1p1f1	0.33	0.33	0.32	16	17	14	47	16
2051-2080	4.5	*Warm and Dry*	HadGEM3-GC31-LL_r1i1p1f3	0.56	0.54	0.59	1	3	3	7	1
			FGOALS_g3_r2i1p1f1	0.29	0.15	0.28	17	27	19	63	20
		Warm and Wet	CanESM5_r9i1p1f1	0.25	0.36	0.30	19	11	16	46	14
			CanESM5_r1i1p1f1	0.17	0.34	0.25	27	16	22	65	21
		Cold and Dry	CNRM-CM6-1_r1i1p1f2	0.35	0.36	0.34	13	13	10	36	11
			MPI-ESM1-2-LR_r3i1p1f1	0.47	0.45	0.47	9	9	8	26	9
			MPI-ESM1-2-LR_r10i1p1f1	0.54	0.55	0.46	5	1	9	15	6
2021-2050	8.5	*Warm and Dry*	HadGEM3-GC31-LL_r1i1p1f3	0.56	0.54	0.59	1	3	3	7	1
			FGOALS-g3_r4i1p1f1	0.25	0.12	0.23	19	28	24	71	24
		Warm and Wet	CanESM5_r3i1p1f1	0.20	0.24	0.27	26	23	21	70	22
			CanESM5_r16i1p1f1	0.17	0.25	0.25	27	21	23	71	24
		Cold and Dry	EC-Earth3-VEG_r1i1p1f1	0.24	0.22	0.19	22	24	26	72	26
			MPI-ESM1-2-LR_r9i1p1f1	0.50	0.52	0.47	8	7	7	22	8
2051-2080	8.5	*Warm and Dry*	HadGEM3-GC31-LL_r1i1p1f3	0.56	0.54	0.59	1	3	3	7	1
			UKESM1-0-LL_r1i1p1f2	0.53	0.48	0.64	6	8	2	16	7
			UKESM1-0-LL_r8i1p1f2	0.53	0.55	0.67	6	2	1	9	5
		Warm and Wet	CanEsm5_r6i1p1f1	0.22	0.25	0.19	24	22	28	74	28
			CanESM5_r9i1p1f1	0.25	0.36	0.30	19	11	16	46	14
		Cold and Dry	EC-Earth3-VEG_r1i1p1f1	0.24	0.22	0.19	22	24	26	72	26
			MPI-ESM1-2-HR_r1i1p1f1	0.36	0.31	0.27	12	19	20	51	18
			MPI-ESM1-2-HR_r2i1p1f1	0.37	0.32	0.29	11	18	18	47	16

Among related studies in Africa, Gebresellase et al. (2022) adopted the advanced envelop-based approach in the Upper Awash basin (UAB) of Ethiopia and selected the skilled models. Similar to their study, this present study also found that MPI_ESM1-2-LR model is skilful in simulating the cold and dry seasons. Moreover, CanESM5 model was selected for having good performance in both studies. Despite having similarities in skilled models, the model differ in their ensemble members.

The selected models runs were downscaled from their coarser resolution to a finer resolution for impact studies.

Table 6 Final selected GCM runs with averaged projected changes in precipitation, mean annual temperature and ETCCDI indices over the study area for the two forcing scenarios (SSP4.5 and SSP8.5) between 2021-2050 and 2051-2080.

Period	SSP	Seasonal Projection	GCM Runs	ΔCDD (%)	Δr95ptot (%)	ΔWSDI (%)	ΔCSDI (%)	ΔT (°C)	ΔP (%)
		Warm and dry	HadGEM3-GC31-LL_r1i1p1f3	-14.4	53.2	5135.7	-13.8	2.1	-1.7
2021-2050	4.5	***Warm and Wet***	CanESM5_r5i1p1f1	-16.1	68.1	3751.4	-92.7	1.9	4.3
		Cold and Dry	MPI_ESM1-2-LR_r5i1p1f1	0.6	-45.3	2398.5	-78.6	0.6	-1.7
		Warm and dry	HadGEM3-GC31-LL_r1i1p1f3	-14.6	52.3	5771.0	-80.6	2.3	-1.1
2051-2080	4.5	***Warm and Wet***	CanESM5_r9i1p1f1	-13.0	69.4	5065.1	-99.0	2.0	5.7
		Cold and Dry	MPI-ESM1-2-LR_r10i1p1f1	2.7	-40.6	3724.9	-98.4	0.5	-1.3
		Warm and dry	HadGEM3-GC31-LL_r1i1p1f3	-16.7	60.9	5792.8	-47.5	3.5	-1.9
2021-2050	8.5	***Warm and Wet***	CanESM5_r3i1p1f1	-9.7	71.3	3903.5	-92.7	2.8	5.6
		Cold and Dry	MPI-ESM1-2-LR_r9i1p1f1	1.4	-40.6	2088.9	-75.7	1.3	-1.5
		Warm and dry	HadGEM3-GC31-LL_r1i1p1f3	-14.0	61.4	6493.5	-95.0	4.5	-1.3
2051-2080	8.5	***Warm and Wet***	CanESM5_r9i1p1f1	-10.4	87.5	6423.7	-100.0	4.2	7.2
		Cold and Dry	MPI-ESM1-2-HR_r2i1p1f1	5.2	-5.2	5103.1	-98.3	2.1	-0.8

4.3 GCM downscaling

Daily GCMs outputs were downscaled for short-term and long-term periods for each climate extreme corners on the 50*50km^2 grid of NCEP-DOE dataset for the Northern Nigeria region (Figure 1). As described in section 3.3, the performance of the three downscaling techniques differs for temperature and precipitation variables. For all the precipitation variables, delta method performs better with higher index of agreement whereas six GCMs were downscaled using EQM and three using QM for the temperature variable.

Precipitation

The study area-raining season follows the West African rainfall characteristics, which prevails during the northern hemisphere summer (June through October). The precipitation is expected to increase in each of the summer months with higher intensities compared to the reference period (Figure 4C and D). For example, an increment of 16% and 23% in June for SSP4.5 and SSP8.5, respectively during the short-term period and a much higher increment of 101% and 102% in October rains is expected during the same period and scenario. Similarly, during the long-term period, the increment is expected in September and October months. An increment of 38% and 81% is expected during SSP4.5 and SSP8.5, respectively in September rains whereas 89% and 148% in October rains for the respective scenarios. Increase in precipitation predicts more rainfall is expected in the future leading to severe flooding events.

Average annual precipitation is also expected to increase for all the GCM models in the future. The average annual precipitation is expected to increase in the future: 8-17% during short-term (CanESM5_r5i1p1f1 predicts highest increase) and 11-35% during long-term (CanESM5_r9i1p1f1 predict highest increase), considering the SSP4.5 scenario. Higher precipitation is expected in the SSP8.5 scenario compared to SSP4.5 scenario because the annual precipitation is expected to increase by 5-38% in short-term (CanESM5_r3i1p1f1 predicts highest increase) and 29-60% in the long-term (CanESM5_r9i1p1f1 predict highest increase) period. Similarly, for the ensemble means (average of 3 GCMs) of the study period, the average annual precipitation is expected to increase in the future: In SSP4.5 during the short-term period, the expected average annual precipitation is 850mm/year yielding a 13% increase with respect to the reference dataset. Likewise, the average annual precipitation (% increase) of 906mm/year (20%), 926mm/year (23%) and 1061mm/year (41%) is expected during long-term (SSP4.5), short-term (SSP8.5) and long-term (SSP8.5) respectively.

The historic, present and future average annual precipitation values of the ensemble mean for SSP4.5 and SSP8.5 for the entire study period with their standard deviations is shown in Figure 5b. In Figure 5b, the dark orange and green lines represent the average values of the annual precipitation while the blue line represent the historic and present average precipitation. The light orange and green areas represent the standard deviation of the average precipitation for SSP4.5 and SSP8.5 respectively. The average annual precipitation values for the reference precipitation variable is 750mm/year.

4.3.2 Temperature

All the GCMs have predicted an increase in temperature with respect to the reference dataset (figure 4A and B). The seasonal increment during the harmattan season (December through February) with respect to the reference dataset varies from 0.2-1.0 C and 1.6-2.4 C for short-term and

long-term periods, considering SSP4.5 scenario. The changes in SSP8.5 is much higher than SSP4.5 scenario with increment of 0.5-1.2 C and 2.0-2.7 C for short-term and long-term period respectively. Increase in harmattan temperature predicts warmer period during the cold season. In the same vein, during the hottest period (March through May), the average monthly mean temperature is expected to increase which varies from 0.2-1.0 C and 1.7-2.7 C for short-term and long-term respectively, considering SSP4.5 scenario. Similarly, and expected increment of 0.3-1.1 C and 2.0-3.0 C for short-term and long-term period, considering SSP8.5 scenario. The rainfall months (June to Spetember) is not an exception to this increment. An increase of 0.9-1.6 C and 2.2-2.8 C is expected for short-term and long-term period respectively, considering SSP4.5 scenario whereas 1.1-1.7 C and 2.3-3.2 C is expected to increase during the short-term and long-term period, considering SSP8.5 scenario. The temperature is expected to increase more compared to hot months and harmattan period.

The average annual mean temperature is expected to increase in the future: 0.26-1.6 C in short-term and 0.87-4.04 C in long-term, considering SSp4.5 scenario. The model CanESM5_r5i1p1f1 is expected to show the highest increment during the short-term while CanESM5_r9i1p1f1 show the highest increment during the long-term period. Higher temperature is expected to increase in SSP8.5 scenario compared to SSp4.5 scenario. The average annual temperature is expected to increase in the short-term by 0.01-1.78 C and 0.01-4.3 C in the long-term period. The model MPI-ESM1-2-LR_r9i1p1f1 and MPI-ESM1-2-HR_r2i1p1f1 show the least increment of 0.01 C whereas HadGEM3-GC31-LL_r1i1p1f3 show the highest increment of both 1.78 C and 4.3 C in the short-term and long-term period respectively.

Similarly, the ensemble mean (average of 3 GCMs) the mean annual temperature is also expected to increase for all the GCMs. In SSP4.5 during the short-term period, the expected increase in mean annual temperature is 1.1 C. Likewise, the mean annual temperature is expected to increase by 2.5 C, 1.2 C and 2.7 C during the long-term (SSP4.5), short-term (SSP8.5), and Long-term (SSP8.5) respectively. The ensemble mean predicts lower temperature increment compared to some of the prediction made by some models, example HadGEM3-GC31-LL_r1i1p1f3.

The historic, present and the future mean annual temperature values of the ensemble means with their standard deviations for SSP4.5 and SSP8.5 for the entire study period is shown in Figure 5a. The dark orange and green lines represent the average values of the mean annual temperature while the blue line represent the historic and the present value. The lighter orange and green areas represent the standard deviations of the mean annual temperature. The mean annual temperature of the reference dataset is 25.6 C.

Conclusion

GCMs are important in climate change assessment. Their outputs are critical for impact studies. Therefore, GCM selection is a vital step before conducting climate change projection studies. Using the advanced envelop-based selection approach, GCMs are selected based on a wide range of multiple criteria for adequate representation of local climate characteristics in Northern Nigeria. Previous impact studies conducted in this region lack multiple selection criteria and are based on random selection of few GCMs. This study provides a clear understanding of the climate characteristics of the region and addresses the limitation in previous studies. In this study, we selected a pool of 100 CMIP6 model output each for SSP4.5 and SSP8.5, making 200 ensemble runs. These models undergo series of selection criteria and the final model representing the study area with outstanding skills were selected. The temperature and precipitation variables of the selected models are downscaled for short-term and long-term periods. Findings from the ensemble mean of the downscaled output during each scenario and study period can be used by river basin authorities for developmental purposes and impact analysis.

The key findings of this research are as follows:

- The changes in precipitation and temperature variables with respect to the reference dataset during the same forcing scenario tends to be higher during the long-term period.
- The changes in precipitation and temperature variables between the GCMs and the reference datasets in the initial step for the short-term ranges from -2.7-4.4% and 0.1-2.7°C respectively for SSP4.5, while for SSP8.5, the ranges are -2.8-5.8% and 0.1-3.5°C respectively.
- Likewise, the changes in precipitation and temperature variables for the long-term period ranges from -2.6-5.7% and 0.3-2.8°C respectively for SSP4.5, whereas the ranges for SSP8.5 are -1.3-7.7% and 0.4-4.5°C.
- The selected skilled GCMs are the same regardless of scenario (SSP4.5 and SSP8.5) as well as the study period (short-term and long-term). The models only exhibit different variant ID.
- CanESM5 models are skilful in capturing the warm and wet seasons of the study area, while HadGEM3_GC3-1_LL are skilful in warm and dry season, whereas MPI-ESM1-2-LR and MPI-ESM1-2-HR are skilful in cold and dry season. Researchers can utilize these models during seasonal analysis.

The downscaled output from the GCMs deduced the following climatic outcome;

- The GCMs predicted and increase in monthly mean temperature during the harmattan, hot and rainfall seasons, with the highest increment during the rainfall season.

- Similarly, the average annual precipitation predicts and increment in the future with more rains in October compared to the reference dataset.
- From the ensemble means of 3 GCMs (1 model from warm and wet, warm and dry and cold and dry corners), the models predict an average annual precipitation of 914mm/year and 918mm/year during the short-term and long-term period respectively, considering SSP4.5, while 906mm/year and 1061mm/year during the short-term and long-term respectively, considering SSP8.5 scenario. Likewise, the ensemble mean of the temperature predicted an increase of 1.1 C and 2.5 C during the short-term and long-term period respectively, considering SSP4.5, while 1.2 C and 2.7 C during the short-term and long-term respectively, considering SSP8.5 scenario.

Ultimately, our study reveals the importance of GCM selection prior to conducting impact studies. The selection is not sensitive to study period and scenarios. Researchers and watershed managers can utilize these models for proper watershed modelling and management.

Statement And Declaration

Funding The authors declare that no funds, grands, or other support were received during the preparation of this study.

Acknowledgement The authors would like to acknowledge the Earth System Grid Federation (ESGF), NCEP DOE, ERA5 and ERA-1 reanalysis for archiving and accessing their dataset.

Author contribution Wada Idris Muhammad contributed to conceptualization, data curation, conducted formal analysis, methodology, coding, investigation, simulation of datasets, results, visualization, writing the original manuscript, review and editing. Haruna Shehu Usman contributed to simulation of data sets, revision, and edited the manuscript. Amechi S. Nwankwegu, Makhai Nwunuji Usman, Selamawit Haftu Gebresellase contributed to review, editing and curation.

Data availability: The full set of raw data and the analysed output that supports the findings of this study are available for future analysis.

Code availability: The codes that support the findings of this study are available from the corresponding author ().

Declarations

Consent for publication: The authors give their consent to the publication of all details of the manuscript, including texts, figures, and tables.

Conflict of interest: The authors declare no competing interests.

References

1. Adakayi, P. E. (2012). An assesment of rainfall and temperature variations in selected stations in parts of Northern Nigeria. In.
2. Aladejana, O. O., Salami, A. T., & Adetoro, O.-I. O. (2018). Hydrological responses to land degradation in the Northwest Benin Owena River Basin, Nigeria. Journal of Environmental Management, *225*, 300–312. doi:10.1016/j.jenvman.2018.07.095
3. Amodu, M., & Ejieji, C. (2017). PERFORMANCE OF SOME GENERAL CIRCULATION MODELS ON PREDICTING TEMPERATURE AND RAINFALL IN THE SUDAN-SAHEL REGION OF NIGERIA. Arid Zone Journal of Engineering, Technology and Environment.
4. Biemans, H., Speelman, L. H., Ludwig, F., Moors, E. J., Wiltshire, A. J., Kumar, P.,.. . Kabat, P. (2013). Future water resources for food production in five South Asian river basins and potential for adaptation — A modeling study. *Science of the Total Environment, 468–469*, S117-S131. doi:https://doi.org/10.1016/j.scitotenv.2013.05.092
5. Chen, H., Xu, C.-Y., & Guo, S. J. J. o. h. (2012). Comparison and evaluation of multiple GCMs, statistical downscaling and hydrological models in the study of climate change impacts on runoff. *434*, 36–45.
6. Eyring, V., Bony, S., Meehl, G. A., Senior, C. A., Stevens, B., Stouffer, R. J., & Taylor, K. E. (2016). Overview of the Coupled Model Intercomparison Project Phase 6 (CMIP6) experimental design and organization. Geosci. Model Dev., *9*(5), 1937–1958. doi:10.5194/gmd-9-1937-2016
7. Fowler, H. J., Blenkinsop, S., & Tebaldi, C. (2007). Linking climate change modelling to impacts studies: recent advances in downscaling techniques for hydrological modelling. International Journal of Climatology, *27*(12), 1547–1578. doi:10.1002/joc.1556
8. Gebresellase, S. H., Wu, Z., Xu, H., & Muhammad, W. I. (2022). Evaluation and selection of CMIP6 climate models in Upper Awash Basin (UBA), Ethiopia. Theoretical and Applied Climatology. doi:10.1007/s00704-022-04056-x
9. Gudmundsson, L., Bremnes, J. B., Haugen, J. E., & Engen-Skaugen, T. (2012). Technical Note: Downscaling RCM precipitation to the station scale using statistical transformations - a comparison of methods. Hydrology and Earth System Sciences, *16*(9), 3383–3390. doi:10.5194/hess-16-3383-2012

10. Hersbach, H., Bell, B., Berrisford, P., Hirahara, S., Horányi, A., Muñoz-Sabater, J.,.. . Thépaut, J.-N. (2020). The ERA5 global reanalysis. *146*(730), 1999–2049. doi:https://doi.org/10.1002/qj.3803
11. Hersbach, H., & Dee, D. (2016). *ERA5 reanalysis is in production, ECMWF Newsletter 147*. https://www.ecmwf.int/en/newsletter/147/news/era5-reanalysis-production
12. Hertig, E., & Jacobeit, J. (2008). Downscaling future climate change: Temperature scenarios for the Mediterranean area. Global Planetary Change, *63*(2–3), 127–131.
13. Jiang, Z., Li, W., Xu, J., & Li, L. (2015). Extreme Precipitation Indices over China in CMIP5 Models. Part I: Model Evaluation %J Journal of Climate. *28*(21), 8603–8619. doi:10.1175/jcli-d-15-0099.1
14. Jin, L., Whitehead, P. G., Appeaning Addo, K., Amisigo, B., Macadam, I., Janes, T.,.. . Rodda, H. J. E. (2018). Modeling future flows of the Volta River system: Impacts of climate change and socio-economic changes. Science of the Total Environment, *637–638*, 1069–1080. doi:https://doi.org/10.1016/j.scitotenv.2018.04.350
15. Kaini, S., Nepal, S., Pradhananga, S., Gardner, T., & Sharma, A. K. (2020). Representative general circulation models selection and downscaling of climate data for the transboundary Koshi river basin in China and Nepal. International Journal of Climatology, *40*(9), 4131–4149. doi:10.1002/joc.6447
16. Kalnay, E., Kanamitsu, M., Kistler, R., Collins, W., Deaven, D., Gandin, L.,.. . Joseph, D. (1996). The NCEP/NCAR 40-Year Reanalysis Project %J Bulletin of the American Meteorological Society. *77*(3), 437–472. doi:10.1175/1520-0477(1996)077<0437:Tnyrp>2.0.Co;2
17. Kanamitsu, M., Ebisuzaki, W., Woollen, J., Yang, S.-K., Hnilo, J. J., Fiorino, M., & Potter, G. L. (2002). NCEP–DOE AMIP-II Reanalysis (R-2) Bulletin of the American Meteorological Society, *83*(11), 1631–1644. doi:10.1175/bams-83-11-1631
18. Katragkou, E., García-Díez, M., Vautard, R., Sobolowski, S., Zanis, P., Alexandri, G.,.. . Jacob, D. (2015). Regional climate hindcast simulations within EURO-CORDEX: evaluation of a WRF multi-physics ensemble. Geosci. Model Dev., *8*(3), 603–618. doi:10.5194/gmd-8-603-2015
19. Kim, B.-S., Kim, B.-K., & Kwon, H.-H. (2011). Assessment of the impact of climate change on the flow regime of the Han River basin using indicators of hydrologic alteration. *25*(5), 691–704. doi:https://doi.org/10.1002/hyp.7856
20. Koutsouris, A. J., Chen, D., & Lyon, S. W. (2016). Comparing global precipitation data sets in eastern Africa: a case study of Kilombero Valley, Tanzania. *36*(4), 2000–2014. doi:https://doi.org/10.1002/joc.4476
21. Lee, J., Sperber, K. R., Gleckler, P. J., Bonfils, C. J. W., & Taylor, K. E. (2019). Quantifying the agreement between observed and simulated extratropical modes of interannual variability. Climate Dynamics, *52*(7), 4057–4089. doi:10.1007/s00382-018-4355-4
22. Li, C., Zhao, T., Shi, C., & Liu, Z. (2021). Assessment of precipitation from the CRA40 dataset and new generation reanalysis datasets in the global domain. *41*(11), 5243–5263. doi:https://doi.org/10.1002/joc.7127
23. Li, M.-H., Tien, W., & Tung, C.-P. (2009). Assessing the impact of climate change on the land hydrology in Taiwan. Paddy and Water Environment, *7*(4), 283. doi:10.1007/s10333-009-0175-9
24. Li, Y. L., Tao, H., Yao, J., & Zhang, Q. (2016). Application of a distributed catchment model to investigate hydrological impacts of climate change within Poyang Lake catchment (China). *Hydrology Research, 47*(S1), 120–135. doi:10.2166/nh.2016.234%J Hydrology Research
25. Lutz, A. F., ter Maat, H. W., Biemans, H., Shrestha, A. B., Wester, P., & Immerzeel, W. W. (2016). Selecting representative climate models for climate change impact studies: an advanced envelope-based selection approach. International Journal of Climatology, *36*(12), 3988–4005. doi:10.1002/joc.4608
26. Maghsood, F. F., Moradi, H., Massah Bavani, A. R., Panahi, M., Berndtsson, R., & Hashemi, H. (2019). Climate Change Impact on Flood Frequency and Source Area in Northern Iran under CMIP5 Scenarios. Water, *11*(2). doi:10.3390/w11020273
27. Maraun, D. (2013). Bias Correction, Quantile Mapping, and Downscaling: Revisiting the Inflation Issue. Journal of Climate, *26*(6), 2137–2143. doi:10.1175/JCLI-D-12-00821.1
28. Maraun, D., Wetterhall, F., Ireson, A. M., Chandler, R. E., Kendon, E. J., Widmann, M.,.. . Thiele-Eich, I. (2010). Precipitation downscaling under climate change: Recent developments to bridge the gap between dynamical models and the end user. *48*(3). doi:https://doi.org/10.1029/2009RG000314
29. Meehl, G. A., Covey, C., Delworth, T., Latif, M., McAvaney, B., Mitchell, J. F. B.,.. . Taylor, K. E. (2007). THE WCRP CMIP3 Multimodel Dataset: A New Era in Climate Change Research. Bulletin of the American Meteorological Society, *88*(9), 1383–1394. doi:10.1175/BAMS-88-9-1383
30. Ndulue, E. L., & Mbajiorgu, C. C. (2019). Modeling climate and land-use change impacts on streamflow and sediment yield of an agricultural watershed using SWAT. Agricultural Engineering International: CIGR Journal, *20*(4), 15–25.
31. O'Neill, B. C., Tebaldi, C., van Vuuren, D. P., Eyring, V., Friedlingstein, P., Hurtt, G.,.. . Sanderson, B. M. (2016). The Scenario Model Intercomparison Project (ScenarioMIP) for CMIP6. Geosci. Model Dev., *9*(9), 3461–3482. doi:10.5194/gmd-9-3461-2016
32. Ogunjo, S. T., Olusegun, C. F., & Fuwape, I. A. (2022). Evaluation of Monthly Precipitation Data from Three Gridded Climate Data Products over Nigeria. Remote Sensing in Earth Systems Sciences. doi:10.1007/s41976-022-00069-2

33. Ometto, J. P., Bun, R., Jonas, M., Nahorski, Z., & Gusti, M. I. (2014). Uncertainties in greenhouse gases inventories – expanding our perspective. Climatic Change, *124*(3), 451–458. doi:10.1007/s10584-014-1149-5
34. Perkins, S. E., Pitman, A. J., Holbrook, N. J., & McAneney, J. (2007). Evaluation of the AR4 Climate Models' Simulated Daily Maximum Temperature, Minimum Temperature, and Precipitation over Australia Using Probability Density Functions. Journal of Climate, *Volume 20*. doi:10.1175/JCLI4253.1
35. Peterson, T. C. (2005). Climate Change Indices. WMO Bulletin, *54*, 83–86.
36. Piani, C., Haerter, J. O., & Coppola, E. (2009). Statistical bias correction for daily precipitation in regional climate models over Europe. Theoretical and Applied Climatology, *99*(1–2), 187–192. doi:10.1007/s00704-009-0134-9
37. Pierce, D. W., Barnett, T. P., Santer, B. D., & Gleckler, P. J. (2009). Selecting global climate models for regional climate change studies. *Proceedings of the National Academy of Sciences, 106*(21), 8441. doi:10.1073/pnas.0900094106
38. Rapaić, M., Brown, R., Markovic, M., & Chaumont, D. (2015). An Evaluation of Temperature and Precipitation Surface-Based and Reanalysis Datasets for the Canadian Arctic, 1950–2010. Atmosphere-Ocean, *53*(3), 283–303. doi:10.1080/07055900.2015.1045825
39. Räty, O., Räisänen, J., & Ylhäisi, J. S. (2014). Evaluation of delta change and bias correction methods for future daily precipitation: intermodel cross-validation using ENSEMBLES simulations. Climate Dynamics, *42*(9), 2287–2303. doi:10.1007/s00382-014-2130-8
40. Sanchez, E., Romera, R., Gaertner, C., Gallardo, C., & Castro, M. (2009). A weighting proposal for an ensemble of regional climate models over Europe driven by 1961–2000 ERA40 based on monthly precipitation probability density functions. ATMOSPHERIC SCIENCE LETTERS. doi:10.1002/asl.230
41. 1002/asl
42. Sawa, B. A., Ati, O. F., Jaiyeoba, I. A., & Oladipo, E. O. (2015). Trends in Aridity of the Arid and Semi-Arid Regions of Northern Nigeria. journal of Environment and Earth Science, *5*, 61–68.
43. Schulzweida, U. (2020). *CDO User Guide (Version 1.9.9)*. In. Retrieved from https://doi.org/10.5281/zenodo.4246983 doi:10.5281/zenodo.4246983
44. Seager, R., Ting, M., Held, I., Kushnir, Y., Lu, J., Vecchi, G.,.. . Naik, N. (2007). Model Projections of an Imminent Transition to a More Arid Climate in Southwestern North America. Science, *316*(5828), 1181. doi:10.1126/science.1139601
45. Shiru, M. S., Chung, E.-S., Shahid, S., & Alias, N. (2020a). GCM selection and temperature projection of Nigeria under different RCPs of the CMIP5 GCMS. Theoretical and Applied Climatology, *141*(3), 1611–1627. doi:10.1007/s00704-020-03274-5
46. Shiru, M. S., Chung, E.-S. J. T., & Climatology, A. (2021). Performance evaluation of CMIP6 global climate models for selecting models for climate projection over Nigeria. *146*(1), 599–615.
47. Shiru, M. S., Shahid, S., Dewan, A., Chung, E.-S., Alias, N., Ahmed, K., & Hassan, Q. K. (2020b). Projection of meteorological droughts in Nigeria during growing seasons under climate change scenarios. Scientific Reports, *10*(1), 10107. doi:10.1038/s41598-020-67146-8
48. Sorg, A., Huss, M., Rohrer, M., & Stoffel, M. (2014). The days of plenty might soon be over in glacierized Central Asian catchments. Environmental Research Letters, *9*(10), 104018. doi:10.1088/1748-9326/9/10/104018
49. Tang, G., Clark, M. P., Papalexiou, S. M., Ma, Z., & Hong, Y. (2020). Have satellite precipitation products improved over last two decades? A comprehensive comparison of GPM IMERG with nine satellite and reanalysis datasets. Remote Sensing of Environment, *240*, 111697. doi:https://doi.org/10.1016/j.rse.2020.111697
50. Tanko, A. I., & Momale, S. B. (2013). *Geography of the Kano Region*. Southbank House Black Prince Road London SE1 7SJ, United Kingdom.: Adonis & Abbey Publishers Ltd.
51. Taylor, K. E. (2001). Summarizing multiple aspects of model performance in a single diagram. *106*(D7), 7183–7192. doi:https://doi.org/10.1029/2000JD900719
52. Taylor, K. E. (2005). Taylor diagram primer. 1–4.
53. Taylor, K. E., Stouffer, R. J., & Meehl, G. A. (2012). An Overview of CMIP5 and the Experiment Design. Bulletin of the American Meteorological Society, *93*(4), 485–498. doi:10.1175/BAMS-D-11-00094.1
54. Umar, D. u. A., Ramli, M. F., Aris, A. Z., Jamil, N. R., & Abdulkareem, J. H. (2018). Runoff irregularities, trends, and variations in tropical semi-arid river catchment. Journal of Hydrology: Regional Studies, *19*, 335–348. doi:https://doi.org/10.1016/j.ejrh.2018.10.008
55. Warszawski, L., Frieler, K., Huber, V., Piontek, F., Serdeczny, O., & Schewe, J. (2014). The Inter-Sectoral Impact Model Intercomparison Project (ISI–MIP): Project framework. *Proceedings of the National Academy of Sciences, 111*(9), 3228. doi:10.1073/pnas.1312330110
56. Werner, A. T., & Cannon, A. J. (2016). Hydrologic extremes – an intercomparison of multiple gridded statistical downscaling methods. Hydrol. Earth Syst. Sci., *20*(4), 1483–1508. doi:10.5194/hess-20-1483-2016
57. Wilby, R. L., Dawson, C. W., & Barrow, E. M. (2002). sdsm — a decision support tool for the assessment of regional climate change impacts. Environmental Modelling & Software, *17*(2), 145–157. doi:https://doi.org/10.1016/S1364-8152(01)00060-3

58. Zhan, W., Guan, K., Sheffield, J., & Wood, E. F. (2016). Depiction of drought over sub-Saharan Africa using reanalyses precipitation data sets. *121*(18), 10,555 – 510,574. doi:https://doi.org/10.1002/2016JD024858
59. Zhang, S., Li, Z., Lin, X., & Zhang, C. (2019). Assessment of Climate Change and Associated Vegetation Cover Change on Watershed-Scale Runoff and Sediment Yield. Water, *11*(7). doi:10.3390/w11071373
60. Zollo, A. L., Turco, M., & Mercogliano, P. (2015). *Assessment of Hybrid Downscaling Techniques for Precipitation Over the Po River Basin*.

Figures

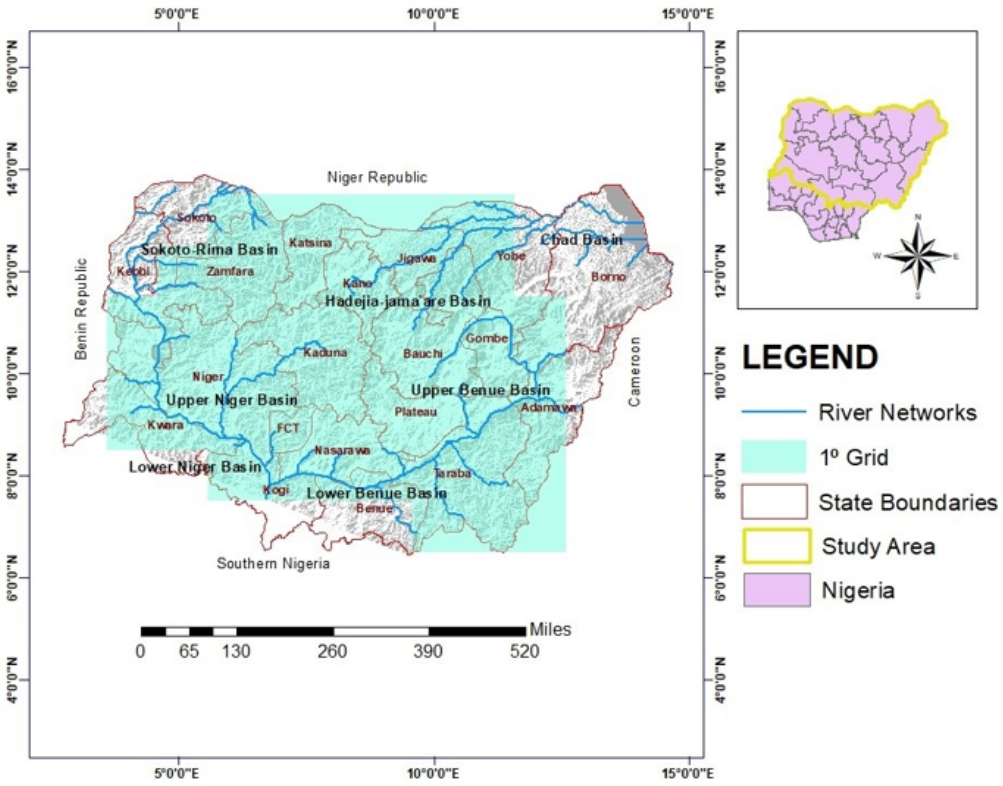

Figure 1

Study area comprising of river basins. The light green colour represents the 1 ×1 grid used for the selection process

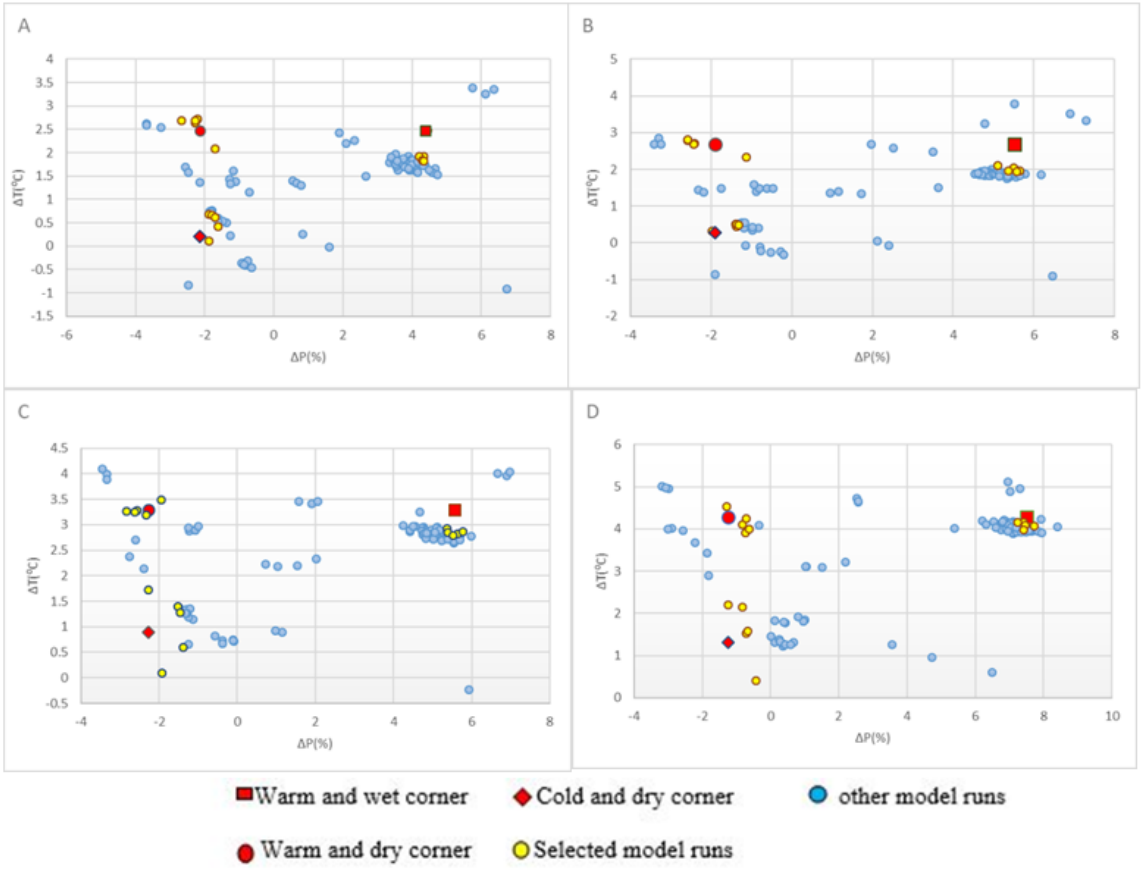

Figure 2: Projected changes based on mean air temperature (ΔT) and annual precipitation sum (ΔP %) between reference period and the projected short-term and long-term period for SSP4.5 (A) and (B) and SSP8.5 (C) and (D) respectively. Red colour shapes indicate the 10th and 90th percentile values for ΔT and ΔP.

Figure 2

See image above for figure legend.

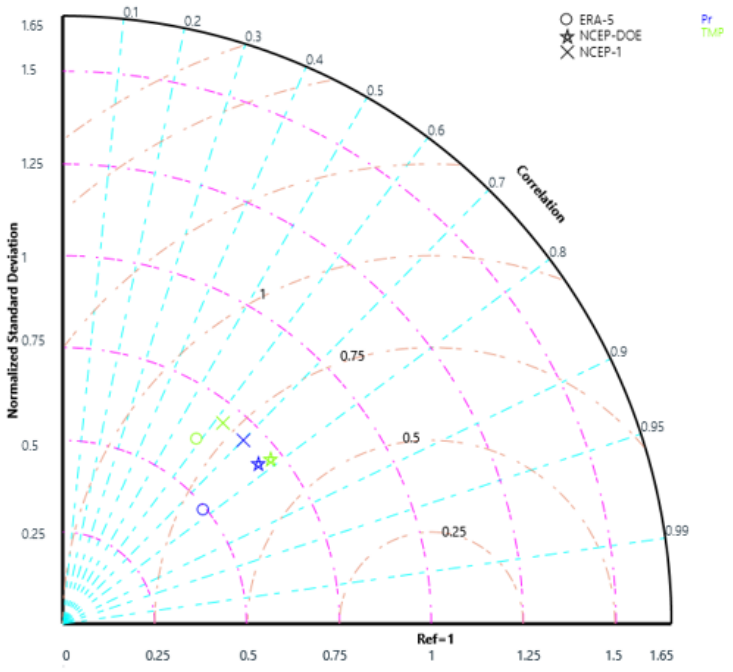

Figure 3

Taylor diagram with blue and lemon colour indicating precipitation and temperature variables respectively.

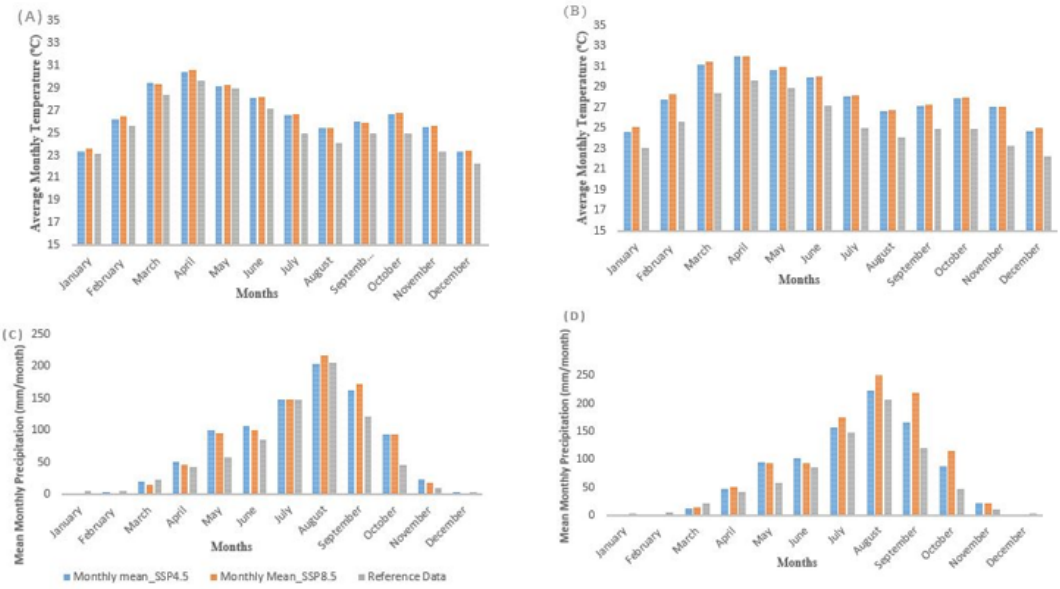

Figure 4

Ensemble mean monthly temperature for short-term and long-term (A and B) and precipitation (C and D) respectively

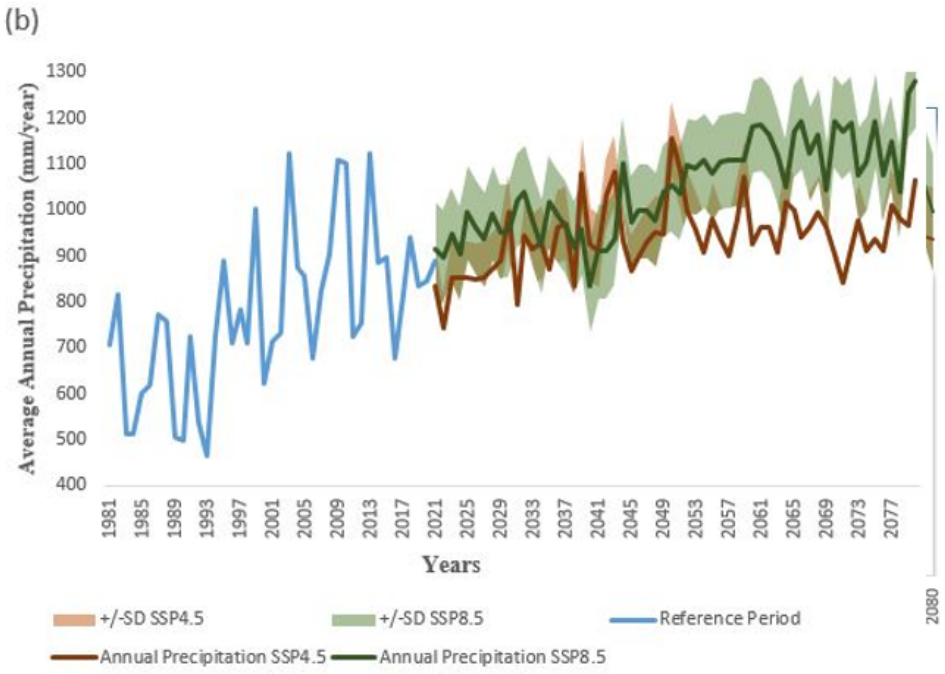

Figure 5

Time series of temperature (a) and precipitation (b) along with their standard deviations for the entire study area